Published in final edited form as:
Ann Biomed Eng. 2007 September ; 35(9): 1485–1497. doi:10.1007/s10439-007-9321-y.

Biochemomechanics of Cerebral Vasospasm and its Resolution:

I. A New Hypothesis and Theoretical Framework

J. D. Humphrey[1], **S. Baek**[2], and **L. E. Niklason**[3]

1*Department of Biomedical Engineering and M.E. DeBakey Institute, Texas A&M University, College Station, TX, USA*

2*Department of Mechanical Engineering, Michigan State University, East Lansing, MI, USA*

3*Departments of Anesthesiology and Biomedical Engineering, Yale University, New Haven, CT, USA*

Abstract

The etiology, and hence most effective treatment, of cerebral vasospasm remains unknown, thus this devastating sequela to subarachnoid hemorrhage continues to be responsible for significant morbidity and mortality. Based on abundant and diverse clinical and laboratory observations, we hypothesize that vasospasm and its subsequent resolution result from a short-term chemo-dominated turnover of cells and matrix in evolving vasoconstricted states that produces a narrowed lumen and thicker wall, which is stiffer and largely unresponsive to exogenous vasodilators, and a subsequent mechano-dominated turnover of cells and matrix in evolving vasodilated states that restores the vessel toward normal. There is, however, a pressing need for a mathematical model of arterial growth and remodeling that can guide the design and interpretation of experiments to test this and competing hypotheses. Toward this end, we present a new biochemomechanical framework that couples a 2-D model of the evolving geometry, structure, and properties of the affected arterial wall, a 1-D model of the blood flow within the affected segment, and a 0-D model of the biochemical insult to the segment. We submit that such a framework can capture salient features of the time-course of vasospasm and its potential resolution, as illustrated numerically in part II of this paper.

Keywords

Subarachnoid hemorrhage; Vasoconstriction; Growth and remodeling; Wall stress; Wall shear stress

INTRODUCTION

Rupture of intracranial aneurysms is the leading cause of non-traumatic subarachnoid hemorrhage (SAH). For those patients who survive to hospitalization, the period 3–7 days post-SAH is critical for it is during this time that there is often a marked short-term reduction in the lumen of, and diminished blood flow within, major cerebral arteries in the vicinity of the hemorrhage. This so-called cerebral vasospasm can occur in up to 70% of patients presenting with SAH and can induce a delayed cerebral ischemia or infarction, thus rendering it the leading cause of morbidity and mortality in these patients. Despite advances in neuroradiology and neurosurgery, effective strategies for treating cerebral vasospasm remain elusive, in large part, because the etiology remains unclear. For more details on the clinical situation, see Macdonald and Weir.[38]

Address correspondence to J. D. Humphrey, Department of Biomedical Engineering, Texas A&M University, 337 Zachry Engineering Center, 3120 TAMU, College Station, TX 77843-3120, USA. Electronic mail: jhumphrey@tamu.edu.

Given the clinical significance of cerebral vasospasm and long-standing recognition of associated alterations in wall structure and vascular smooth muscle contractility,[45] it is remarkable that there has been no attempt to formulate a biomechanical framework for analysis. Mathematical models can help guide the identification and interpretation of new experiments, aid in the evaluation of competing hypotheses on the underlying mechanisms, and direct the design of new clinical treatments. In this paper, we propose a simple biochemomechanical framework that is motivated by a new hypothesis for cerebral vasospasm. We hypothesize that vasospasm and its potential resolution result from an acute vasoconstriction due to the initial bleed, a short-term chemo-dominated growth and remodeling (G&R) process that progresses in evolving vasoconstricted states in response to the developing extravascular clot and produces a narrowed lumen and thicker wall, which is stiffer and largely unresponsive to exogenous vasodilators, and finally a mechano-dominated G&R process that progresses in evolving vasodilated states in response to the dissolution of the clot and restores the vessel toward normal (Fig. 1). By G&R, we mean a turnover and/or reorganization of cells and extracellular matrix that can alter the overall mass and microstructure of the arterial wall. Indeed, we hypothesize further that this turnover of structurally significant constituents in evolving vasoaltered states yields new constituents that have new natural (i.e., stress-free) configurations, mass fractions, and possibly orientations, but otherwise similar biomechanical properties (e.g., new collagen fibers have the same intrinsic stiffness); these changes can alter both the material and the structural stiffness of the wall about the smaller lumen. Although there will be a need to identify specific constitutive relations, our goal is to show that this overall framework can capture salient features of the pathophysiology of cerebral vasospasm and thereby can be used to set new directions for basic research and possibly clinical intervention.

EMPIRICAL OBSERVATIONS

Normal arterial development as well as subsequent functional adaptations, responses to injury, and many disease processes appear to occur via similar means—a cell mediated turnover of wall constituents at different rates, to different extents, and in different biomechanical states.[23] It is because of the diverse repertoire of cellular activities (e.g., migration, proliferation, apoptosis, synthesis or degradation of matrix, and the production of adhesion molecules, vasoactive molecules, growth factors, and cytokines), however, that there are so many different manifestations of arterial G&R. For example, the lumen of a normal artery enlarges in response to sustained increases in blood flow, the thickness of the wall increases in response to sustained increases in blood pressure, the length of a vessel increases in response to sustained increases in axial load, the wall experiences neointimal hyperplasia in cases of damage to the endothelium and internal elastic lamina, and so on.[14,33,35]

Understanding cerebral vasospasm within the context of arterial G&R is complicated by the co-existence of many different synergistic and competitive processes (e.g., see reviews by Mayberg *et al*.,[40,41] Dietrich and Dacey,[12] Macdonald,[37,38] McGirt *et al*.,[42] Dumont *et al*.,[13] Zhang *et al*.,[65] Grasso,[19] Pluta,[53] Zhang and Macdonald[66] and copious references therein). Here, we attempt to summarize, synthesize, and interpret some of the many reported observations, which suggest the aforementioned hypothesis for the progression and resolution of vasospasm. It appears, for example (Fig. 2), that the organizing extravascular clot causes a marked increase in vasoconstrictors (e.g., serotonin (5-HT), thromboxane (TXA_2), endothelin-1 (ET-1), and thrombin) and increase in scavengers (e.g., reactive oxygen species, oxyhemoglobin) of nitric oxide (NO, a potent vasodilator). This initial shift toward more constrictors causes an acute, likely maximal, net vasoconstriction. The presence of multiple clot related mitogens (e.g., platelet derived growth factor (PDGF), transforming growth factor (TGF-β), and ET-1) appears to promote the proliferation and possible migration of medial smooth muscle cells and adventitial fibroblasts in evolving vasoconstricted states as well as possibly to cause changes in the smooth muscle that favors a leftward shift in the active force

—length curve and the synthesis of additional collagen; whereas proliferation and synthesis may increase the mass and thickness of the wall, and consequently the structural stiffness, the shift in the force—length curve may exacerbate the initial vasoconstriction. An extreme constriction, in turn, may disrupt endothelial cells due to corrugation of the intima (cf. Fig. 1 in Mayberg *et al.*[40] or Fig. 7 in Handa *et al.*[20]) which could decrease endothelial production of NO and prostacyclin (PGI_2, an inhibitor of platelet aggregation and a mild vasodilator) as well as decrease its responsiveness to endogenous or exogenous circulating vasodilators. Moreover, endothelial damage could increase permeability as well as upregulate multiple adhesion and chemotactic molecules (e.g., vascular cell adhesion molecule (VCAM-1) and monocyte chemoattractant protein (MCP-1)) that promote both inflammatory (involving cytokines such as the interleukins (IL-1, IL-6, IL-8) and tissue necrosis factor (TNF-α)) and degradatory (via macrophages and production of matrix metalloproteinases (MMP-1, MMP-2, MMP-9)) responses by sequestering and activating lymphocytes and mononuclear phagocytes. Together, therefore, the extravascular blood clot and endothelial disruption appear to set into motion a heightened G&R of the arterial wall in evolving vasoconstricted states, one that includes a phenotypic modulation of smooth muscle cells that promotes increased turnover of cells and extracellular matrix.[62] This leads to a narrowed lumen and thickened wall (i.e., a stiffer structure) with a small increase in cross-sectional area but an increase in collagen mass fraction (i.e., a stiffer material). Such a net change in geometry, active and passive mechanical properties, and perivascular constraints (possibly including the mass effect of the organizing clot and an increased intracranial pressure) would feedback to change further the biology of the wall, which appears to be dominated by chemo-stimuli early on. As the clot dissolves and the endothelium recovers, however, it appears that the altered biomechanics, particularly a decreased intramural stress (which may promote atrophy of the thickened wall; cf. Bayer *et al.*[5]) and an increased wall shear stress (which may stimulate the production of vasodilators such as NO, platelet inhibitors such as PGI_2, and growth factors such as vascular endothelial derived growth factor, VEGF[11,35]), both relative to normal/homeostatic values, may allow the mechano-stimuli to dominate again, such that a flow-induced G&R in vasodilated states can restore the lumen toward normal. The vessel may thus begin to return to its prior geometry and properties via a turnover of constituents in these evolving vasodilated states. Clinically, such recovery may take 4 weeks or more if the patient survives the severe effects that may initiate between 3 and 7 days and peak between 5 and 12 days post-SAH.

We submit that the variable time-courses of change from primarily mechano-dominated to chemo-dominated control, and back, with growth and remodeling occurring in rapidly evolving states based on perturbations from different basal rates of turnover (due, e.g., to age dependency) and differently cross-linked extracellular matrices (due, e.g., to disease status related to diabetes or smoking) contribute to the diverse observations that have been reported on the patho-physiology and efficacy of particular clinical treatments. In other words, part of the extreme variability in clinical presentation may be due to the evolving nature of the process —one's observation will depend strongly on the time from the SAH, its severity, and individual rates of turnover in evolving states, which likely vary considerably from patient to patient. Other factors, which can either exacerbate or attenuate the effects of the focal vasospasm, include the location of the bleed within the cerebral circulation and the associated ability of distal resistance beds to autoregulate, the presence of a distal collateral circulation, and overall changes in intracranial pressure and circulation of cerebrospinal fluid.[36]

We are not the first to suggest that cerebral vasospasm is yet another manifestation of arterial G&R, nor are we the first to suggest that there is a critical interplay between vasoactive and remodeling responses. For example, Mayberg *et al.*[40,41] suggested years ago that "cerebral arteriopathic changes after SAH may represent one component of a common vascular response to injury, which may be mediated by similar processes" and that "structural changes may act in concert with contractile mechanisms to alter normal physiologic responses and maintain a

narrowed lumen." We are, however, the first to suggest a specific means by which such G&R can occur and to suggest a novel theoretical framework that can begin to account for and synthesize these many diverse observations for purposes of describing and predicting time-courses.

THEORETICAL FRAMEWORK

Notwithstanding the incredible complexity of the biochemical and biomechanical processes that lead to cerebral vasospasm and its possible resolution, it is prudent to begin with simple mathematical models. Yet, our growing understanding of vascular mechanics and mechanobiology demands that we consider coupled effects of wall mechanics and hemodynamics as well as the effects of diverse vasoregulatory, mitogenic, and proteolytic molecules that are associated with the development and dissolution of an extravascular blood clot. As a compromise between biochemical/biomechanical complexity and mathematical simplicity, we employ a "2-D model" of G&R mechanics of the arterial wall (i.e., we focus on the mean pressure-induced circumferential wall stress σ_θ and mean axial load-induced wall stress σ_z). Moreover, we employ a "1-D model" of flow in a cylindrical vasospastic segment within a dual-path network model of the cerebral vasculature, and focus on the time-averaged mean transmural pressure P and flow-induced wall shear stress τ_w (by 1-D, we imply that the pressure and velocities depend only on axial position along the segment or network). Finally, although one could use reaction—diffusion equations to describe the development and dissolution of a spatially distributed clot and its products,[30,64] we focus on the net concentration of the primary effector molecules presented to the wall. That is, we consider a "0-D model" of the time-varying ratio C of the concentrations of constrictors to dilators (i.e., spatially uniform chemical reactions within the 2-D wall). It is important to note, therefore, that there are two very different time scales: we average changes over a cardiac cycle (time scale of seconds), but we account directly for changes during the progression and resolution of vasospasm (time scale of weeks, with this time denoted as t). When data are available on mechanobiological responses in terms of pulsatility, such effects can be included naturally (cf. Olufsen *et al.*[49] and Alastruey *et al.*[1] who discuss distal flow boundary conditions). Let us now consider each of these aspects of the formulation separately.

Biosolid Mechanics

Consistent with the use of time-averaged mean values of the luminal pressure and wall shear stress, we consider quasi-static wall mechanics[25] within a 2-D framework.[17] Overall equilibrium of the arterial wall requires that the mean in-plane Cauchy stresses within a cylindrical vasospastic segment (Fig. 2) balance the applied transmural pressure P (i.e., luminal pressure P_v minus cerebrospinal fluid pressure P_{CSF}) and the applied axial force f, namely[27]

$$\sigma_\theta(t) = \frac{P(t)\,a(t)}{h(t)}, \sigma_z(t) = \frac{f(t)}{\pi h(t)(2a(t)+h(t))}, \forall t, \tag{1}$$

where a and h are the inner radius and wall thickness in loaded states. Homeostatic (i.e., normal) values of these stresses, σ_θ^h and σ_z^h, appear to be in the order of 100 kPa for both directions in arteries such as common carotids and basilars.[21,26] Note that these equations are determined by statics alone, independent of constitutive relations for the stress response in terms of deformations. To understand potential changes in wall properties over time, however, we must consider the constitutive behavior.

G&R Mechanics

We recently proposed a constrained mixture theory to describe arterial G&R[24] and showed that associated 2-D models capture salient features of flow- and pressure-induced adaptations in arteries[17,18] as well as aspects of the enlargement of intracranial aneurysms.[2] Because our ultimate motivation is the clinical situation, for which one needs primarily to understand the evolution of the lumen and the structural stiffness of the wall, we similarly adopt a 2-D approach to study the progression and potential resolution of the vasospasm.

The fundamental hypothesis is that arterial G&R occurs via the different rates and extents of turnover of individual, structurally significant constituents within altered states. There is, therefore, a need to track changes in the deformations, mass fractions, and orientations of individual constituents. Consistent with concepts from membrane theory[23] and prior work on aneurysms,[2] we postulate a constrained mixture constitutive relation for principal tensions (i.e., stresses multiplied by the wall thickness h) in the vasospastic wall as:

$$\begin{aligned} T_\theta(t) &= \frac{1}{\lambda_z(t)} \frac{\partial}{\partial \lambda_\theta(t)} \left(\sum w^i(t) \right) + h(t)\, \sigma_\theta^{\text{act}}(t), \\ T_z(t) &= \frac{1}{\lambda_\theta(t)} \frac{\partial}{\partial \lambda_z(t)} \left(\sum w^i(t) \right), \end{aligned} \tag{2}$$

where w^i is the strain-energy stored in each structurally significant constituent i, per surface area relative to an experimentally accessible mixture reference configuration, $\sigma_\theta^{\text{act}}$ is the active stress due to smooth muscle contraction, which is typically assumed to be in the circumferential direction, and (λ_θ, λ_z) are experimentally measurable principles stretches are experienced by the vessel. Together, Eqs. (1) and (2) require that, at any G&R time t,

$$\begin{aligned} &\frac{1}{\lambda_z(t)} \sum \frac{\partial w^i}{\partial \lambda_\theta(t)} + h(t)\, \sigma_\theta^{\text{act}}(t) = P(t)\, a(t), \\ &\frac{1}{\lambda_\theta(t)} \sum \frac{\partial w^i}{\partial \lambda_z(t)} = \frac{f(t)}{\pi(2a(t)+h(t))}, \end{aligned} \tag{3}$$

where i will typically denote elastin, smooth muscle fibers, or collagen fibers (k = 1,2,…, n families of locally parallel collagen fibers, or generically c), thus $i = e, m, c$.

Before discussing the requisite strain-energy functions, consider the standard forward problem in solid mechanics. If we know constitutive relations for the individual constituents as well as the evolution of their natural configurations, mass fractions, and orientations, and if we can either prescribe or measure the applied loads $P(t)$ and $f(t)$, then these two coupled algebraic equations (3) represent, at each G&R time t, two governing equations in terms of three key kinematic parameters: deformed radius, wall thickness, and length (i.e., a, h, l). Clearly, we need an additional equation at each time t. Although there can be marked changes in the mass fractions (i.e., $\phi^i = \rho^i/\rho$) of structurally significant constituents, the overall mass density $\rho = \sum \rho^i$ of a soft tissue appears to change little during many manifestations of G&R.[56] Hence, letting V denote the total volume of the vasospastic segment, the constraint of a constant overall mass density of the wall (i.e., $\sigma(t) \cong \sigma(0)$) requires that

$$\left.\begin{aligned} \rho(t)\, V(t) &= \alpha(t)\, \bar{M}_o \\ \rho(0)\, V(0) &= \bar{M}_o \end{aligned}\right\} \alpha(t) = \frac{\pi h(t)\,(2a(t)+h(t))\,\ell(t)}{\pi h(0)\,(2a(0)+h(0))\,\ell(0)}, \tag{4}$$

where $\bar{M}_o$ is the original total mass of the segment and $\alpha(t)$ is a gross measure of overall growth ($\alpha > 1$) or atrophy ($\alpha < 1$), with $\alpha(0) \equiv 1$. If the overall growth or atrophy is known (e.g., segment

volume given a constant overall mass density), then we have three equations (two equilibrium equations represented by Eq. (3) plus a mass density constraint represented by Eq. (4)) to solve simultaneously for our three primary unknowns (a, h, l) in a forward problem at each time t, provided the applied loads are known or measurable.

We ultimately seek to use this theoretical framework to study the time-course of vasospasm in patients and thereby to facilitate the design of improved clinical interventions, yet we will see that this will require data that are not currently available. Until and even after such data are available, simulations based on representative data, illustrative constitutive relations, and special cases can be used to study consequences of competing hypotheses or potential clinical interventions. For example, consider the special case wherein an arterial segment maintains its length throughout the progression and resolution of vasospasm, $l(t) \equiv l(0)$, that is, the vessel does not become tortuous. In this case, the mass density constraint becomes

$$\alpha(t)\,(h(0)\,(2a(0)+h(0))) \equiv \delta(t) = h^2(t) + 2a(t)\,h(t)\,, \tag{5}$$

where values at time 0 may be estimated from normal contralateral vessels in the circle of Willis. Hence, we can solve for either $a(t)$ or $h(t)$ at any G&R time t in terms of $\delta(t)$. For example,

$$h(t) = +\sqrt{a^2(t) + \delta(t)} - a(t)\,, \tag{6}$$

where the term within the radical equals the outer radius squared. In this case, our three coupled equations for the wall reduce to two uncoupled equations in terms of two unknowns: $a(t)$, which is determined by solving Eq. $(3)_1$, and $f(t)$, which can then be determined directly from Eq. $(3)_2$. Indeed, whereas the *in vivo* pressure can be inferred from hemodynamic computations, or potentially measured directly, the *in vivo* axial force cannot be so determined. This emphasizes the need to track potential length changes *in vivo* (which could be accomplished by tracking the separation distance between branch sites distal and proximal to the vasospastic segment) to support or replace the assumption of a constant length.

Let us now address further the metric $\alpha(t)$, and consider the critically important kinetics of cell and matrix turnover. Again following Baek *et al.*,[2] the total mass density of the mixture, defined per reference area at time t, can be calculated by knowing how much of each constituent was produced at past times plus their half lives. Specifically, let the current mass density of the mixture (i.e., vasospastic segment) be

$$\begin{aligned} M(t) &= \sum M^i(t)\,, \\ M^i(t) &= M^i(0)\,Q^i(t) + \int_0^t m^i(\tau)\,q^i(t,\tau)\,d\tau, \end{aligned} \tag{7}$$

where $M^i(0)$ is the original mass density of constituent i, $Q^i(t)$ is the fraction of constituent i that was produced prior to time 0 (when the initial bleed occurred) and survives to time t, $m^i(\tau)$ is the rate at which constituent i is produced (i.e., mass density production) following the initial bleed, which may vary with time depending on chemomechanical conditions including wall shear and intramural stress, and $q^i(t, \tau)$ is the survival function for constituent i, which describes how much of the material produced at time $\tau \in [0, t]$ survives to time t. Consequently, $\alpha(t) = M(t)/M(0)$, thus completing Eq. (5).

A general form for the strain-energy function for a structurally significant constituent i, as needed in Eq. (3), can be written similarly as (generalized from Baek *et al.*[2])

$$w^i(t) = \frac{M^i(0)}{\rho} Q^i(t)\, W^i\left(\mathbf{F}^i_{\mathrm{n}(0)}(t)\right) + \int_0^t \frac{m^i(\tau)}{\rho} q^i(t,\tau)\, W^i\left(\mathbf{F}^i_{n(\tau)}(t)\right) d\tau, \tag{8}$$

where W^i is a constituent-specific strain-energy function defined, per unit volume, relative to a computationally convenient reference configuration. $\mathbf{F}^i_{\mathrm{n}(\tau)}(t) = \partial \mathbf{x}(t) / \partial \mathbf{X}^i(\tau)$ is the deformation gradient at time t for constituent i, which was produced at time τ and thus has a natural (stress-free) configuration defined at time τ; it is computed by assuming that the motion of each structurally significant constituent is constrained to equal that of the vessel as a whole although the natural configuration of a constituent is allowed to evolve separately over instants of production τ. Because $Q^i(0) \equiv 1$ by definition, Eq. (8) recovers the classical rule-of-mixtures relation at $t = 0$ as it should. Finally, note that the heredity integral is similar to that in viscoelasticity; with continual turnover, material produced in the recent past will survive longer and thus contribute more to load bearing than material produced in the distant past.

Cerebral arteries contain little elastin.[34] Regardless of amount, structurally significant vascular elastin tends not to turnover in maturity,[33] thus we may assume that it can be damaged and/or degraded, but it cannot be produced anew or at least not properly cross-linked if produced. In this case, $m^{\mathrm{e}}(\tau) = 0$ ($i = e$) and

$$w^{\mathrm{e}}(t) = \frac{M^{\mathrm{e}}(0)}{\rho} Q^{\mathrm{e}}(t)\, W^{\mathrm{e}}\left(\mathbf{F}^{\mathrm{e}}_{\mathrm{n}(0)}(t)\right). \tag{9}$$

In contrast, we may assume that there is significant turnover (i.e., production and removal, which need not balance) of smooth muscle and collagen. Assuming further that both the passive smooth muscle and the collagen exist locally as parallel constituents, we can let each family of "fibers" be considered as an individual constituent. For example, with circumferentially oriented smooth muscle,[60]

$$w^{\mathrm{m}}(t) = \frac{M^{\mathrm{m}}(0)}{\rho} Q^{\mathrm{m}}(t)\, W^{\mathrm{m}}\left(\lambda^{\mathrm{m}}_{\theta,\mathrm{n}(0)}(t)\right) + \int_0^t \frac{m^{\mathrm{m}}(\tau)}{\rho} q^{\mathrm{m}}(t,\tau)\, W^{\mathrm{m}}\left(\lambda^{\mathrm{m}}_{\theta,\mathrm{n}(\tau)}(t)\right) d\tau, \tag{10}$$

whereas for $k = 1,2,\ldots n$ families of collagen fibers having diverse directions in the θ—z plane,[22]

$$\begin{aligned} w^{\mathrm{c}}(t) &= \sum_k w^k(t) \\ &= \sum_k \left(\frac{M^k(0)}{\rho} Q^k(t)\, W^k\left(\lambda^k_{n(0)}(t)\right) \right. \\ &\quad \left. + \int_0^t \frac{m^k(\tau)}{\rho} q^k(t,\tau)\, W^k\left(\lambda^k_{n(\tau)}(t)\right) d\tau, \right. \end{aligned} \tag{11}$$

where $W^k\left(\lambda^k_{\mathrm{n}(\tau)}(t)\right)$ represents the energy stored in the kth collagen fiber family, which in turn depends on the stretch experienced by those fibers. This stretch is determined by the current deformation at time t as well as the associated natural (or stress-free) configuration that existed at the time τ that the constituent was produced. For example, if we let the deposition (i.e., homeostatic) stretch of a particular collagen fiber family be given by G^k_{h}, then

$$\lambda^k_{\mathrm{n}(\tau)}(t) = G^k_{\mathrm{h}} \frac{\lambda^k(t)}{\lambda^k(t)}, \lambda^k(t) = \sqrt{\left(\lambda_z \cos \alpha^k_{\mathrm{o}}\right)^2 + \left(\lambda_\theta \sin \alpha^k_{\mathrm{o}}\right)^2}, \tag{12}$$

where α^k_{o} denotes the angle between the axial direction of the vessel and the fiber direction in a common reference configuration. Further details can be found in Baek *et al.*[2]

Information is yet insufficient for detailed modeling of the active stress—stretch behavior of vascular smooth muscle, but we know that there is typically a sigmoidal dose—response curve whereby increasing concentrations of constrictors induce greater force generation and *vice versa* for dilators.[52] Likewise, there is a nonlinear stress—stretch response whereby force generation increases with increasing stretch until a maximum stretch (say λ_{M}, which may evolve with G&R) is attained, after which there is diminished force generation with increasing stretch; moreover, there is a value of stretch (say λ_{o}, which may also evolve) below which force generation ceases. Based on these general observations, and building on the work of Rachev and Hayashi,[54] one can assume an active stress response for the smooth muscle of the form

$$\sigma^{\mathrm{act}}_\theta(t) = T_{\mathrm{M}} \tilde{f}(C(t)) \int \widehat{f}\left(\lambda^{\mathrm{m}}_{\theta,\mathrm{n}(\tau)}(t); \lambda_{\mathrm{M}}, \lambda_{\mathrm{o}}\right) d\tau, \tag{13}$$

where T_{M} is the maximum stress-generating capacity of smooth muscle[43] (~200 kPa), $C(t)$ is the aforementioned ratio of the concentration of constrictors over dilators, $\tilde{f}(C) \in [0, \quad 1]$ represents a normalized sigmoidal dose—response behavior, and $\lambda^{\mathrm{m}}_{\theta,\mathrm{n}(t)}$ is the circumferential stretch of smooth muscle that was produced at instant τ. This model can capture salient features of the activation, but it does not account for the likely multiaxial character of smooth muscle contraction and it does not account for a possible stretch-sensitivity to agonists.[52] It will need to be refined as data become available.

Biofluid Mechanics

Equations (1) to (13) reveal that, in addition to standard biosolid mechanical information, there is a need for information on the luminal pressure and wall shear stress. Because these quantities may change during the progression and resolution of vasospasm, they must come from a coupled solution of the hemodynamics. In particular, the pressure in the lumen of the vasospastic segment P_{v} contributes directly to the circumferential equilibrium equation for the wall; P_{v} is expected to decrease as the vasospasm progresses, then increase as the vasospasm resolves. The state of muscle activation, and hence overall equilibrium, depends on the ratio of constrictors to dilators C, which in turn depends in part on flow-induced wall shear stress τ_{w} (e.g., increased τ_{w} upregulates the production of NO by the normal endothelium and decreased τ_{w} upregulates the production of ET-1).[11] Wall shear stress is expected to increase as the vasospasm progresses, then decrease as it resolves. Finally, rates of mass production and removal, that is $m^i(\tau)$ and $q^i(t, \tau)$, may depend on the wall shear stress (e.g., ET-1 is smooth muscle mitogen and promoter of collagen production) and luminal pressure (which dictates intramural wall stress and hence collagen production), not just the overall chemical environment.

The Reynolds number within large arteries of the cerebral circulation is typically less than 500 (Fernandez *et al.*[15]) thus suggesting a laminar flow. The mean value of wall shear stress within the central region of the vasospastic segment can thus be approximated as[27]

$$\tau_w = \frac{4\mu Q}{\pi a^3}, \tag{14}$$

where μ is the absolute viscosity of the flowing blood, Q is the local volumetric flowrate, and a is the inner radius of the cylindrical vessel in its distended configuration; of course, $Q = \pi a^2 v$ where v is the mean velocity. The homeostatic value of wall shear stress τ_w^h appears to be in the order of 3–6 Pa in the cerebral circulation.[9,44]

Various clinical metrics define the severity of vasospasm. These include angiographically measured reductions in the lumen (e.g., graded as mild if < 25% reduction in luminal diameter, moderate if ~25–50% reduction, and severe if > 50% reduction)[29,65] and transcranial doppler measured increases in mean velocity within the vasospastic segment (e.g., vasospasm is implicated by a mean velocity in the middle cerebral artery, MCA, > 120 cm/s, a 24-h increase in MCA velocity > 50 cm/s, or a ratio of the velocity in the MCA to the internal carotid artery, ICA, of MCA:ICA > 3).[58] Because these metrics are related via Q, they simply represent different clinical preferences based on available data.

Reports of mean velocity before and after vasospasm often reveal increases of 100% or more (e.g., increased MCA velocity from ~60 to 160 cm/s), with effiective therapies targeting comparable percent reductions.[50] Blood flow depends on the pressure gradient that drives the flow, which ultimately depends on arterial P_A vs. capillary P_C pressures. Such pressure drops (P_A — P_C) can be approximated in 1-D using a control volume energy equation by accounting for “losses” in the network. Whereas one typically considers simple viscous and geometric losses in a tube flow,[63] the presence of a complex plexus of distal autoregulating resistance vessels complicates such an analysis in the cerebral circulation. It is common, therefore, to introduce a lumped parameter model for the resistance vessels. For example, Olufsen *et al.*[49] model the resistance using a binary fractal tree approach whereas Ferrandez *et al.*[15] model the resistance using Darcy’s law for flow in a porous media. Regardless of the specific approach, a lumped parameter model of the distal resistance can be coupled with a control volume analysis of the vasospastic segment (Fig. 3). Note, too, that Lodi and Ursino[36] modeled the many large vessels that constitute the circle of Willis (e.g., anterior cerebral, middle cerebral, posterior cerebral, basilar, and communicating arteries) and their distal beds as a “dual-path” network: flow is partitioned between those vessels that are normal and that vessel which is vasospastic (Fig. 4). This allows a straightforward implementation of a combined energy equation/lumped parameter resistance model, which will be adopted herein. Lodi and Ursino suggested further that four key biomechanical factors govern the hemodynamics in cerebral vasospasm: the severity of the vasospastic constriction, degree of autoregulation, increase in intracranial pressure, and presence of distal collaterals. They showed, for example, that the presence of both distal collaterals and autoregulating resistance vessels can dramatically reduce the effects of focal vasospasm whereas increased intracranial pressure exacerbates the devastating effects. The potential effects of collaterals will not be addressed here, however.

The governing equations for a two-path network are mass balance (i.e., assuming incompressibility, the total flow in must balance the total flow out) and energy balance (e.g., the pressure drop is the same along each path), namely[51]

$$Q = Q_n + Q_v \text{ and } \left(\frac{P_A - P_C}{\rho_f}\right)_n = \left(\frac{P_A - P_C}{\rho_f}\right)_v, \tag{15}$$

where subscripts n and v denote the normal and vasospastic paths, respectively, and subscripts *A* and *C* denote arterial and capillary pressures common to each pathway; σ_f is the mass density of the fluid (blood, assumed to be constant). The control volume energy equation for flow between any two points 1 (upstream) and 2 (downstream) in a tube is[27]

$$\left(\frac{P_1}{\rho_f}+\frac{1}{2}\alpha_f v_1^2\right)-\left(\frac{P_2}{\rho_f}+\frac{1}{2}\alpha_f v_2^2\right)=\sum\left(F_f\frac{\ell}{d}\frac{v^2}{2}+K_f\frac{v^2}{2}\right), \tag{16}$$

where α_f, F_f, and K_f are, respectively, the kinetic energy coefficient ($\alpha_f = 2$ for a laminar flow), the friction factor ($F_f = 64/Re$ for a laminar flow, where the Reynolds number is $Re = \sigma_f v d/\mu$), and the minor loss coefficient for a change in geometry (K_f typically equals 0.5 or less for gradual contractions and expansions); l is a generic length of the tube over which viscous losses occur and d (=2a) is its diameter. Alternatively, a pressure drop ΔP and associated volumetric flow Q can be related through a lumped resistance R, namely $\Delta P = RQ$. It can be shown that, consistent with Figs. 3 and 4 wherein we consider a vasospastic segment within a middle cerebral artery, Eq. $(15)_2$ can be written as:

$$\begin{aligned} R_n Q_n = {} & \frac{8\mu\ell_o(1-x)}{a_o^2}\left(\frac{Q_v}{\pi a_o^2}\right)+\frac{8\mu\ell_o x}{a_v^2}\left(\frac{Q_v}{\pi a_v^2}\right) \\ & +K_f\rho_f\left(\frac{Q_v}{\pi a_v^2}\right)^2+R_v Q_v, \end{aligned} \tag{17}$$

where R_n is the total lumped resistance in the normal path (large and small vessels), a_o and a_v are radii in the vasospastic segment before and during vasospasm ($a_v \equiv a$ in the biosolid mechanics formulation), x is the percentage of the original length l_o that narrows ($x l_o \equiv l$ in the biosolid mechanics formulation), and R_v is the lumped resistance for beds distal to the vasospastic segment (in this case a MCA).

Here, consider two possible cases. First, if the total cerebral flow Q is unchanging and known, then Eqs. (17) and $(15)_1$ represent two equations in terms of the two unknown flows; they yield a simple quadratic equation for Q_v, the solution of which allows Q_n to be determined and thus how the total blood flow Q partitions. That is,

$$Q_v=\frac{-B\pm\sqrt{B^2-4AC}}{2A}, Q_n=Q-Q_v, \tag{18a}$$

where

$$\begin{aligned} A &\equiv \frac{K_f}{\pi^2 a_v^4}, \\ B &\equiv \frac{8\mu\ell_o(1-x)}{\pi\rho_f a_o^4}+\frac{8\mu\ell_o x}{\pi\rho_f a_v^4}+\frac{R_v}{\rho_f}+\frac{8\mu\ell_n}{\pi\rho_f a_n^4}+\frac{R_n}{\rho_f}, \\ C &\equiv -\frac{8\mu\ell_n}{\pi\rho_f a_n^4}-\frac{R_n}{\rho_f}. \end{aligned} \tag{18b}$$

Second, we can determine Q_n directly from the left-hand side of Eq. $(15)_2$ given the pressure drop for the normal path (P_A) — P_C) and similarly determine Q_v directly from the right-hand side of Eq. $(15)_2$ given (P_A — P_C) for the vasospastic path. In this second case, total cerebral flow Q may decrease due to an overall increased resistance to flow (e.g., impaired autoregulation). Specifically,

$$Q_{\mathrm{n}}=\frac{P_{\mathrm{A}}-P_{\mathrm{C}}}{R_{\mathrm{n}}},Q_{\mathrm{v}}=\frac{-B\pm\sqrt{B^2-4AC_P}}{2A}, \tag{19a}$$

where

$$\begin{aligned} A &\equiv \frac{K_{\mathrm{f}}\rho_{\mathrm{f}}}{\pi^2 a_{\mathrm{v}}^4}, B\equiv \frac{8\mu\ell_{\mathrm{o}}(1-x)}{\pi a_{\mathrm{o}}^4}+\frac{8\mu\ell_{\mathrm{o}}x}{\pi a_{\mathrm{v}}^4}+R_{\mathrm{v}},\\ C_P &\equiv P_C-P_{\mathrm{A}}. \end{aligned} \tag{19b}$$

Finally, given the input arterial pressure P_{A} to both paths and the value of the flow through the vasospastic segment, Eq. (16) determines the luminal pressure in the center of the segment, namely

$$\begin{aligned} P_{\mathrm{v}}=P_{\mathrm{A}} &-\tfrac{1}{2}\alpha_{\mathrm{f}}\rho_{\mathrm{f}}\left(v_{\mathrm{v}}^2-v_{\mathrm{o}}^2\right)-\frac{4\mu\ell_{\mathrm{o}}(1-x)}{a_{\mathrm{o}}^2}v_{\mathrm{o}}\\ &-\tfrac{1}{2}K_{\mathrm{f}}\rho_{\mathrm{f}}v_{\mathrm{v}}^2-\frac{4\mu\ell_{\mathrm{o}}x}{a_{\mathrm{v}}^2}v_{\mathrm{v}}, \end{aligned} \tag{20}$$

with $v_{\mathrm{v}}=Q_{\mathrm{v}}/\pi a_{\mathrm{v}}^2$ and $v_{\mathrm{o}}=Q_{\mathrm{v}}/\pi a_{\mathrm{o}}^2$. Hence, by solving these simple hemodynamic equations, we can determine the mean luminal pressure and wall shear stress that are needed in the G&R equations for the vasospastic wall. Recall, however, that it is the transmural pressure $P(t) = P_{\mathrm{v}}(t) — P_{\mathrm{CSF}}(t)$ that enters the equilibrium equation, where t is the G&R time not the time during a cardiac cycle, hence reminding us that the intracranial pressure also needs to be measured or prescribed as a function of the progression and resolution of the vasospasm. Finally, let us consider effects of the evolving clot.

Chemomechanics

Many vasoactive substances are associated with normal arterial biology (e.g., vasodilators NO and PGI_2 and vasoconstrictors ANG-II and ET-1), but a SAH presents the arterial wall with many more substances, particularly vasoconstrictors (e.g., thrombin as well as platelet-derived serotonin (5-HT) and thromboxane (TXA_2)—see Fig. 2), and clinical treatment may introduce yet other substances that are designed to affect vasoactivity (e.g., papavarine, calcium channel blockers, or ET_A and ET_B receptor blockers). Eventually, the kinetics of production, activation, and inhibition of all clot-produced molecules need to be quantified and included in a G&R framework. Here, however, we begin by focusing on overall vasoconstriction or vasodilatation, and thus the overall imbalance between constrictors and dilatators as well as receptor sensitivity or availability. Motivated thus, consider a time-dependent net concentration $C(t)$ of constrictors over dilators presented to the wall to be given by

$$\begin{aligned} C(t)= &\ C_{\mathrm{basal}}(\xi(t))+C_{\mathrm{myogenic}}(t)-C_{\mathrm{shear}}(\xi(t))\\ &+C_{\mathrm{clot}}(t)-C_{\mathrm{treatment}}(\xi(t)). \end{aligned} \tag{21}$$

Contributors to basal tone are a normal flow-induced production of NO or ET-1 and the autonomic nervous system; the former can be compromised by endothelial damage, however, which can be modeled via a damage function $\xi(t) \in [0, 1]$ with $\xi = 1$ denoting no damage and $\xi = 0$ denoting complete damage (i.e., loss of function). Cerebral arteries exhibit a mild myogenic response, but this could be neglected in an initial model given the paucity of data on the associated mechanics and because the intraluminal pressure is expected to reduce only slightly due to vasospasm (see Eq. 20). Changes in tone due to changes in wall shear stress

from baseline are due primarily to changes in the production of NO and ET-1, with dilation correlating with increases in wall shear stress above homeostatic values and constriction correlating with decreases below homeostatic values in a normal endothelium.[11] Constrictor molecules associated with the formation of a clot were noted above and clearly play the central role in the progression and resolution of the vasospasm; there is a pressing need for descriptors of the time-course of changes in clot related vasoactive molecules and their effects, which could be accomplished by solving appropriate systems of reaction—diffusion equations, but here we model only the final net effect. Finally, clinical treatment could include the infusion of potent vasodilators (e.g., papaverine) that may or may not work through the endothelium. Such pharmacologic therapy could be administered either as a bolus injection (modeled via an exponential decay) or as a continuous infusion over time (approximated via a beta function), but we do not consider such treatments here.

In summary, Eqs. (1) to (21) represent the first biochemomechanical framework for modeling cerebral vasospasm. Although the consequence of vasospasm is a diminished blood flow, the cause is a modification of the arterial wall. Hence, the three primary equations are the two equilibrium equations and the mass density constraint for the wall (Eqs. 3 and 4), which by incorporating G&R relations (e.g., Eqs. 7–13) allow one to solve for the evolving geometry (radius, length, and thickness) and stiffiness in terms of evolving loads (e.g., blood pressure) and material properties (strain-energy functions, which depend on mass production and removal). The ratio of constrictors to dilators (Eq. 21), which depends on the fluid shear stress and hence the volumetric flow, enters the equilibrium equations through both the muscle contraction term and mass density production terms (constrictors are mitogens); the fluid pressure enters directly into the circumferential equilibrium equation for the wall as an applied load; and, of course, the changing arterial geometry affiects the hemodynamics, which in turn affiect the production of vasoactive molecules. Hence, the solids, fluids, and chemical insult are fully coupled, and the equations will require iterative solution.

Although a detailed understanding of the biomechanics and pathophysiology of cerebral vasospasm may require much more complex modeling, including 3-D wall mechanics and hemodynamics, we submit that this simple theoretical framework provides new guidance as to what ought to be measured and it will allow competing hypotheses and potential clinical treatments to be contrasted numerically. Illustrative constitutive relations and model simulations are reported in a companion paper (part II; Baek *et al*.[3]).

DISCUSSION

There is an extensive literature on cerebral vasospasm and many different treatment strategies have been evaluated, including calcium channel blockers, triple-H therapy (hypertensive/hypervolemic/hemodilution), intra-arterial infusion of papaverine, and balloon angioplasty.[19,65,67] Nevertheless, this complex sequela of a SAH largely remains a clinical enigma. In order for the present theoretical framework to be used to explore potential hypotheses, mechanisms, or treatments, there is a pressing need for specific data as revealed by the various constitutive functions. For example, there is a need for information on the possible evolution of endothelial damage $\xi(t)$, effects due to the development and dissolution of the clot $C_{\text{clot}}(t)$, the material properties of the wall constituents ($\sigma_\theta^{\text{act}}(t)$ and $w^i(t)$), and of course the rates of production $m^i(\tau)$ and removal $q^i(t, \tau)$ of wall constituents. Here, let us consider some of the information in the literature that can be used in this regard.

The frequent resistance of vasospastic arteries to potent vasodilators has long implicated structural changes within the wall.[28,40,61,66] It is remarkable, therefore, that few investigators have quantified evolving changes in the mechanical properties of arteries due to the progression of vasospasm. Nagasawa *et al*.[45] reported marked leftward shifts in both the passive and active

pressure—diameter curves of human cerebral arteries collected at autopsy 7–10 days post-SAH; in particular, they reported significant stiffening in the potassium-induced active response, which implied a heightened contractility. Data from autopsy tissue must be interpreted cautiously, however, given that tissue was not collected until well after death. In a nice follow-up study, Nagawasa *et al*.[46,47] reported histological and mechanical data at 0, 2, 4, 7, 14, and 28 days post-SAH in a canine model. Significant amounts of clotted blood were found around the basilar artery at 2 and 4 days, with the hematoma decreasing thereafter such that no clot was detectable at 28 days. Such data are useful for determining the function $C_{\text{clot}}(t)$, as are clinical data from CT (Reilly *et al*.[55]), the latter of which suggests further the need to know the half-life of the molecules released by the clot or their long term effects.[6]

A significant increase in extracellular matrix proteins, especially collagen, suggests an overall trend toward fibrosis and medial necrosis, which provides some information related to the forms of $m^i(\tau)$ and $q^i(t, \tau)$ and consequently the overall metric of wall growth or atrophy $\alpha(t)$. Nagawasa *et al*. also reported that vessel contractility was heightened at 2, 4, 7, and 14 days post-SAH, but especially at 7 days; they wrote, “the contractile capacity of the wall itself increases with the advance of vasospasm,” at least during initial stages. Such information can be useful in constructing forms for $\sigma_\theta^{\text{act}}(t)$, which evolve due to smooth muscle turnover. See, too, Bakker *et al*.[4] and Martinez-Lemus *et al*.[39] Such findings are supported in part by the study by Butler *et al*.,[8] who reported that “Vasospastic arterial segments had greater passive tension and greater intrinsic tone than did controls.” Kim *et al*.[31] also reported a decreased distensibility, an increase in resting tension, and a decrease in the minimum stretch at which smooth muscle generates force actively following SAH, which they suggested favored a smaller diameter vessel. Yamaguchi-Okada *et al*.[62] reported a progressive decrease in the contribution of smooth muscle activation and concomitant increase in passive stiffness over 7–28 days following SAH in a canine model, findings that correlated well with measured changes in smooth muscle differentiation markers and matrix composition. Our hypothesis that new tissue is produced and organized in vasoaltered configurations so as to preserve a preferred constituent stretch (or stress) is consistent with many of these observations, which can aid in postulating forms for $w^i(t)$, yet the need for more detailed data on time—course of change is clear.

That a heightened turnover of constituents contributes to rapid G&R of the wall is supported directly by the reported presence of multiple smooth muscle mitogens, growth factors, and proteases,[7,12,37,68] noting that vasoconstrictors also tend to be mitogens. Moreover, our hypothesis is supported indirectly by the observation by Torbey *et al*.[57] that vasospasm is more likely in younger patients. Whereas turnover rates can increase many-fold in response to altered-mechanical loads and chemical stimuli,[59] it is becoming increasingly evident that such turnover occurs much faster in younger people.[10,32]

Although 3-D computational fluid dynamics models can be developed for the cerebral circulation[9,44] and 3-D analyses can be formulated for arterial G&R,[24] it is prudent to begin with simpler models that build intuition, that allow one to test basic competing hypotheses more efficiently, and that may be more useful clinically. Our 1-D fluid mechanical modeling is consistent with the majority of the current work on cerebral hemodynamics,[15,16,48] including the only related work to date on cerebral vasospasm[36]; our 2-D solid mechanical modeling of an adapting wall has been shown to recover salient features in diverse circumstances[2,17,18] and is sufficient for modeling changes in clinically important parameters such as geometry and structural stiffness. We submit, therefore, that the present theoretical framework is a reasonable first approach to modeling the progression and resolution of cerebral vasospasm and it is sufficiently general to incorporate diverse data as they become available. Nevertheless, the biofluid mechanics and biochemical kinetics could be rendered much more sophisticated while supplying the same requisite information (luminal pressure, wall shear

stress, and net effect of constrictors vs. dilators) to the growth and remodeling model of the wall. The key, however, is the need for more data, which is also revealed better by the present framework.

In summary, it appears that a SAH sets into motion a rapid shift from a normal mechano-dominated vasoactivity and maintenance of wall properties to a chemo-dominated change in vasoactivity and turnover of intramural constituents in evolving states, with a delayed return to mechano-dominated control as the clot dissolves. In particular, it appears that multiple vasoconstrictors associated with the organizing clot induce an acute, maximum vasoconstriction, which because of an associated marked increase in mitogens and cytokines results in a heightened turnover of intramural constituents in evolving vasoaltered states. Such G&R, coupled with additional vasoconstriction, leads to an artery having a smaller lumen and dysfunctional endothelium as well as a thicker, stiffier wall that is largely unresponsive to exogenous vasodilators during the critical, early period post-SAH. As the clot dissolves and the damaged endothelium recovers, however, the balance shifts back toward normal mechano-dominated control with the decreased intramural stresses promoting atrophy of the thickened wall and the increased wall shear stress in the narrowed vessel tending to cause the artery to dilate; this causes the artery to remodel in successive dilated states, thereby restoring the vessel toward normal (provided the patient survives the early chemo-dominated changes). This hypothesis is separate from a particular mathematical model, of course, and should be explored both numerically (see part II) and experimentally.

A key advantage of a theoretical framework is that it can guide the design and interpretation of experiments as well as the collection of clinical data. The biochemomechanical framework presented herein reveals that there is a need for basic information (e.g., time-course of changes in cerebral blood flow, arterial, capillary, and CSF pressures, distal resistances, properties of the normal wall) and local information related to the vasospasm (e.g., length of the affiected segment, extent of the bleed, autoregulatory impairment). In addition, if we are to have predictive capability, there is a need for a better understanding of basal and accelerated turnover rates (e.g., changes in the mass density production rates $m^k(\tau)$ in response to the bleed, and the survival functions $q^k(t, \tau)$ associated with this newly produced material). Such functions must come from laboratory studies that track time-dependent changes in structurally significant constituents such as collagen, elastin, and smooth muscle[62] as well as various clot-related growth factors, cytokines, and MMPs. Such data are beginning to become available in other areas of arterial mechanics (e.g., balloon-induced damage, flow- and pressure-induced remodeling), but there is a pressing need for such data for cerebral vasospasm. Given the associated significant mortality and morbidity, collection of these data must be given a high priority.

ACKNOWLEDGMENTS

This work was supported by NIH grants HL-80415 and HL-64372 (through the Bioengineering Research Partnership Program).

REFERENCES

1. AlastrueyJParkerKHPeiroJByrdSMSherwinSJModelling the circle of Willis to assess the effects of anatomical variations and occlusions on cerebral flows. J. Biomech (in press).
2. Baek S, Rajagopal KR, Humphrey JD. A theoretical model of enlarging intracranial fusiform aneurysms. ASME J. Biomech. Eng 2006;128:142–149.
3. BaekSValentinAHumphreyJDBiomechanics of cerebral vasospasm and its resolution: II. Constitutive relations and model simulations. Ann. Biomed. Eng doi: 10.1007/s10439-007-9322-x.

4. Bakker ENTP, Buus CL, VanBavel E, Mulvaney MJ. Activation of resistance arteries with endothelin-1: from vasoconstriction to functional adaptation and remodeling. J. Vasc. Res 2004;41:174–182. [PubMed: 15017111]
5. Bayer IM, Adamson SL, Langille BL. Atrophic remodeling of the artery-cuffed artery. Arterioscler. Thromb.Vasc. Biol 1999;19:1499–1505. [PubMed: 10364081]
6. Bermek H, Peng KC, Angelova K, Ergul A, Puett D. Endothelin degradation by vascular smooth muscle cells. Reg. Peptides 1996;66:155–162.
7. Borel CO, McKee A, Parra A, Haglund MM, Solan A, Prabhakar V, Sheng H, Warner DS, Niklason LE. Possible role for vascular cell proliferation in cerebral vasospasm after subarachnoid hemorrhage. Stroke 2003;34:427–433. [PubMed: 12574555]
8. Butler WE, Peterson JW, Zervas NT, Morgan KG. Intracellular calcium, myosin light chain phosphorylation, and contractile force in experimental cerebral vasospasm. Neurosurgery 1996;38:781–788. [PubMed: 8692399]
9. Cebral JR, Castro MA, Soto O, Lohner R, Alperin N. Blood flow models of the circle of Willis from magnetic resonance data. J. Eng. Math 2003;47:369–386.
10. Clerin V, Nichol JW, Petko M, Myung RJ, Gaynor JW, Gooch KJ. Tissue engineering of arteries by directed remodeling of intact arterial segments. Tissue Eng 2003;9:461–472. [PubMed: 12857414]
11. Davies PF. Flow-mediated endothelial mechanotransduction. Physiol. Rev 1995;75(3):519–560. [PubMed: 7624393]
12. Dietrich HH, Dacey RG. Molecular keys to the problems of cerebral vasospasm. Neurosurgery 2000;46:517–530. [PubMed: 10719847]
13. Dumont AS, Dumont RJ, Chow MM, Lin C-L, Calisaneller T, Ley KF, Kassell NF, Lee KS. Cerebral vasospasm after subarachnoid hemorrhage: putative role of inflammation. Neurosurgery 2003;53:123–135. [PubMed: 12823881]
14. Dzau VJ, Gibbons GH. Vascular remodeling: mechanisms and implications. J. Cardiovasc. Pharmacol 1993;21(Suppl):S1–S5. [PubMed: 7681124]
15. Ferrandez A, David T, Brown MD. Numerical models of auto-regulation and blood flow in the cerebral circulation. Comput. Meth. Biomech. Biomed. Eng 2002;5:7–20.
16. Gao E, Young WL, Pile-Spellman J, Ornstein E, Ma Q. Mathematical considerations for modeling cerebral blood flow autoregulation to systemic arterial pressure. Am. J. Physiol 1998;274:H1023–H1031. [PubMed: 9530217]
17. Gleason RL, Taber LA, Humphrey JD. A 2-D model of flow-induced alterations in the geometry, structure and properties of carotid arteries. ASME J. Biomech. Eng 2004;126:371–381.
18. Gleason RL, Humphrey JD. A mixture model of arterial growth and remodeling in hypertension: Altered muscle tone and tissue turnover. J. Vasc. Res 2004;41:352–363. [PubMed: 15353893]
19. Grasso G. An overview of new pharmacological treatments for cerebrovascular dysfunction after experimental subarachnoid hemorrhage. Brain Res. Dev 2004;44:49–63.
20. Handa Y, Hayashi M, Takeuchi H, Kuubota T, Kobayashi H, Kawano H. Time course of the impairment of cerebral autoregulation during chronic cerebral vasospasm after subarachnoid hemorrhage in primates. J. Neurosurg 1993;78:112–119. [PubMed: 8416225]
21. Hu JJ, Fossum TW, Miller MW, Xu H, Liu S, Humphrey JD. Biomechanical behavior of the porcine basilar artery in hypertension. Ann. Biomed. Eng 2007;35:19–29. [PubMed: 17066325]
22. HuJJBaekSHumphreyJDStress–strain behavior of the passive basilar artery in normotension and hypertension. J. Biomech (in press).
23. Humphrey, JD. Cells, Tissues, and Organs. Springer-Verlag; NY: 2002. Cardiovascular Solid Mechanics.
24. Humphrey JD, Rajagopal KR. A constrained mixture model for arterial adaptations to a sustained step change in blood flow. Biomech. Model Mechanobiol 2003;2:109–126. [PubMed: 14586812]
25. Humphrey JD, Na S. Elastodynamics and arterial wall stress. Ann. Biomed. Eng 2002;30:509–523. [PubMed: 12086002]
26. Humphrey JD, Wilson E. A potential role of smooth muscle tone in early hypertension: a theoretical study. J. Biomech 2003;36:1595–1601. [PubMed: 14522200]

27. Humphrey, JD.; Delange, SL. Analysis and Design. Springer-Verlag; NY: 2004. An Introduction to Biomechanics: Solids and Fluids.
28. Kapp JP, Neill WR, Neill CL, Hodges LR, Smith RR. The three phases of vasospasm. Surg. Neurol 1982;18:40–45. [PubMed: 7112386]
29. Kassell NF, Helm G, Simmons N, Phillips CD, Cail WS. Treatment of cerebral vasospasm with intra-arterial papaverine. J. Neurosurg 1992;77:848–852. [PubMed: 1432125]
30. Khanin MA, Semenov VV. A mathematical model of the kinetics of blood coagulation. J. Theor. Biol 1989;136:127–134. [PubMed: 2779263]
31. Kim P, Sundt TM, Vanhoutte PM. Alterations of mechanical properties in canine basilar arteries after subarachnoid hemorrhage. J. Neurosurg 1989;71:430–436. [PubMed: 2769393]
32. Langille BL, Bendeck MP, Keeley FW. Adaptations of carotid arteries of young and mature rabbits to reduced carotid blood flow. Am. J. Physiol 1989;256:H931–H939. [PubMed: 2705563]
33. Langille BL. Arterial remodeling: relation to hemodynamics. Can. J. Physiol. Pharmacol 1996;74(7): 834–841. [PubMed: 8946070]
34. Lee RMKW. Morphology of cerebral arteries. Pharmac. Ther 1995;66:149–173.
35. Levy, BI.; Tedgui, A. Kluwer Academic Press; Dordrecht: 1999. Biology of the Arterial Wall.
36. Lodi CA, Ursino M. Hemodynamic effect of cerebral vasospasm in humans: a modeling study. Ann. Biomed. Eng 1999;27:257–273. [PubMed: 10199702]
37. Macdonald RL. Pathophysiology and molecular genetics of vasospasm. Acta Neurochir 2001;77:7–11.
38. Macdonald, RL.; Weir, B. Academic Press; San Diego: 2001. Cerebral Vasospasm.
39. Martinez-Lemus LA, Hill MA, Bolz SS, Pohl U, Meininger GA. Acute mechanoadaptation of vascular smooth muscle cells in response to continuous arteriolar vasoconstriction: implications for functional remodeling. FASEB J 2004;18:708–710. [PubMed: 14977879]
40. Mayberg MR, Okada T, Bark DH. Morphologic changes in cerebral arteries after subarachnoid. Neurosurg. Clinics N Am 1990;1:417–432.
41. Mayberg MR, Okada T, Bark DH. The significance of morphological changes in cerebral arteries after subarachnoid hemorrhage. J. Neurosurg 1990;72:626–633. [PubMed: 2319321]
42. McGirt MJ, Lynch JR, Blessing R, Warner DS, Friedman AH, Laskowitz DT. Serum von Willebrand factor, matrix metalloproteinase-9, and vascular endothelial growth factor levels predict the onset of cerebral vasospasm after aneurysmal subarachnoid hemorrhage. Neurosurgery 2002;51:1128–1135. [PubMed: 12383357]
43. Milnor, WR. Oxford University Press; 1990. Cardiovascular Physiology.
44. Moore S, David T, Chase JG, Arnold J, Fink J. 3D models of blood flow in the cerebral vasculature. J. Biomech 2005;39:1454–1463. [PubMed: 15953607]
45. Nagasawa S, Handa H, Okumura A, Naruo Y, Okamoto S, Moritake K, Hayashi K. Mechanical properties of human cerebral arteries: part 2. Vasospasm. Surg. Neurol 1980;14:285–290. [PubMed: 7434196]
46. Nagasawa S, Handa H, Naruo Y, Moritake K, Hayashi K. Experimental cerebral vasospasm arterial wall mechanics and connective tissue composition. Stroke 1982;13:595–600. [PubMed: 7123591]
47. Nagasawa S, Handa H, Naruo Y, Watanabe H, Moritake K, Hayashi K. Experimental cerebral vasospasm. Part 2. Contractility of spastic arterial wall. Stroke 1983;14:579–584. [PubMed: 6658935]
48. Olufsen MS, Peskin CS, Kim WY, Pedersen EM, Nadim A, Larsen J. Numerical simulation and experimental validation of blood flow in arteries with structured-tree outflow conditions. Ann. Biomed. Eng 2000;28:1281–1299. [PubMed: 11212947]
49. Olfusen MS, Nadim A, Lipsitz LA. Dynamics of cerebral blood flow regulation explained using a lumped parameter model. Am. J. Physiol 2002;282:R611–R622.
50. Oskouian RJ Jr, Martin NA, Lee JH, Glenn TC, Guthrie D, Gonzalez NR, Afari A, Vinuela F. Multimodal quantitation of the effects of endovascular therapy for vasospasm on cerebral blood flow, transcranial doppler ultrasonographic velocities, and cerebral artery diameters. Neurosurgery 2002;51:30–41. [PubMed: 12182433]
51. Potter, MC.; Wiggert, DC. Prentice Hall; Englewood Cliffs, NJ: 1991. Mechanics of Fluids.

52. Price JM, Davis DL, Knauss EB. Length-dependent sensitivity in vascular smooth muscle. Am. J. Physiol 1981;241:H557–H563. [PubMed: 7315980]
53. Pluta RM. Delayed cerebral vasospasm and nitric oxide: Review, new hypothesis, and proposed treatment. Pharmacol. Therapeut 2005;105:23–56.
54. Rachev A, Hayashi K. Theoretical study of the effects of vascular smooth muscle contraction on strain and stress distributions in arteries. Ann. Biomed. Eng 1999;27:459–468. [PubMed: 10468230]
55. Reilly C, Amidei C, Tolentino J, Jahromi BS, Macdonald RL. Clot volume and clearance rate as independent predictors of vasospasm after aneurysmal subarachnoid hemorrhage. J. Neurosurg 2004;101:255–261. [PubMed: 15309916]
56. Rodriguez EK, Hoger A, McCulloch AD. Stress-dependent finite growth in soft elastic tissues. J. Biomech 1994;27:455–467. [PubMed: 8188726]
57. Torbey MT, Hauser T-K, Bhardwaj A, Williams MA, Ulatowski JA, Mirski MA, Razumovsky AY. Effect of age on cerebral blood flow velocity and incidence of vasospasm after aneurysmal subarachnoid hemorrhage. Stroke 2001;32:2005–2011. [PubMed: 11546889]
58. Vajkoczy P, Horn P, Bauhuf C, Munch E, Hubner U, Ing D, Thome C, Poeckler-Schoeninger C, Roth H, Schmiedek P. Effect of intra-arterial papaverine on regional cerebral blood flow in hemodynamically relevant cerebral vasospasm. Stroke 2001;32:498–505. [PubMed: 11157189]
59. ValentinAHumphreyJDOn time-courses of cell and matrix turnover in arterial remodeling . (submitted).
60. Walmsley JG, Campling MR, Chertkow HM. Interrelationships among wall structure, smooth muscle orientation, and contraction in human major cerebral arteries. Stroke 1983;14:781–790. [PubMed: 6197786]
61. Weaver JP, Fisher M. Subarachnoid hemorrhage: an update of pathogenesis, diagnosis and management. J. Neurolog. Sci 1994;125:119–131.
62. Yamaguchi-Okada M, Nishizawa S, Koide M, Nonaka Y. Biomechanical and phenotypic changes in the vasospastic canine basilar artery after subarachnoid hemorrhage. J. Appl. Physiol 2005;99:2045–2052. [PubMed: 16051708]
63. Young DF. Fluid mechanics of arterial stenoses. ASME J. Biomech. Eng 1979;101:157–175.
64. Zarnitsina VI, Pokhilko AV, Ataullakhanov FI. A mathematical model for the spatio-temporal dynamics of intrinsic pathway of blood coagulation. I The model description. Thrombosis Res 1996;84:225–236.
65. Zhang B, Fugleholm K, Day LB, Ye S, Weller RO, Day INM. Molecular pathogenesis of subarachnoid haemorrhage. Int. J. Biochem. Cell Biol 2003;35:1341–1360. [PubMed: 12798348]
66. Zhang Z-D, Macdonald RL. Contribution of the remodeling response to cerebral vasospasm. Neurol. Res 2006;28:713–720. [PubMed: 17164034]
67. Zubkov YN, Nikiforov BM, Shustin VA. Balloon catheter technique for dilatation of constricted cerebral arteries after aneurysmal SAH. Acta Neurochir 1984;70:1–2.
68. Zuccarello M. Endothelin: the “prime suspect” in cerebral vasospasm. Acta Neurochir 2001;77:61–65.

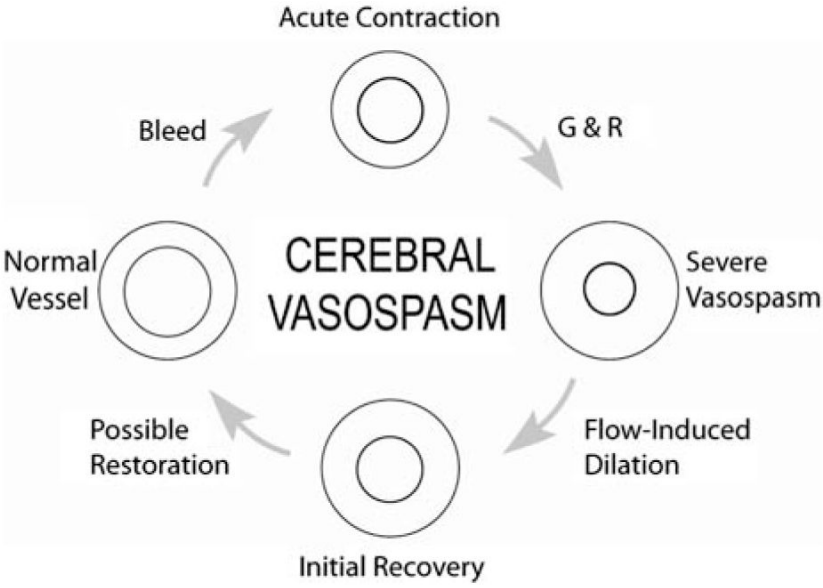

FIGURE 1.

Schema of the progression and possible resolution of cerebral vasospasm following a SAH: the initial bleed causes an acute contraction, turnover of cells and matrix in evolving vasoconstricted states yields the severe vasospasm, and turnover of cells and matrix in evolving vasodilated states may restore the vessel back toward normal. Indeed, shown, too, is a possible continuation to a near complete restoration. Albeit not indicated, the time-courses of these phases differ considerably: the acute contraction may initiate within minutes to hours, the G&R in evolving vasoconstricted states likely occurs over the first 3–10 days, and the subsequent dilation-induced G&R likely occurs over the next 20 or more days. Hence, vasospasm often peaks between 5 and 12 days and, if the person survives, it often resolves nearly completely by 28 days.

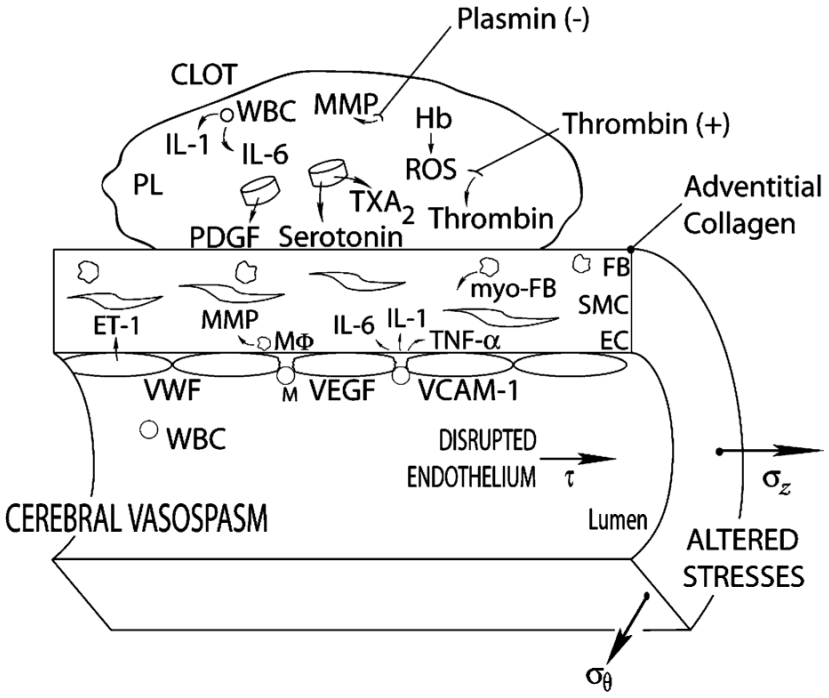

FIGURE 2.

Schema of a few of the many molecules involved in the development and dissolution of an extravascular clot. In particular, note the key role played by thrombin, which converts fibrinogen to fibrin (and thereby promotes the organization of the clot) and activates platelets (which produce multiple vasoconstrictors and growth factors). Indeed, although thrombin can promote endothelial production of NO, it also has a direct vasoconstrictor effect on smooth muscle. Note, too, that oxyhemoglobin (oxyHb) in the clot can scavenge NO, and the production of other reactive oxygen species (ROS) exacerbates such scavenging. Finally, the clot is eventually degraded via the action of plasmin. Shown, too, are the mean in-plane biaxial stresses (circumferential and axial) as well as the flow-induced wall shear stress; the effect of the shear stress on the wall mechanobiology will depend on whether the endothelium is disrupted or not by the severe constriction. The endothelium may also alter its production of adhesion molecules (e.g., VCAM-1), which in turn will affect the recruitment of monocytes (M) to the wall and thus possible invasion of macrophages (Mφ), which produce additional proteases.

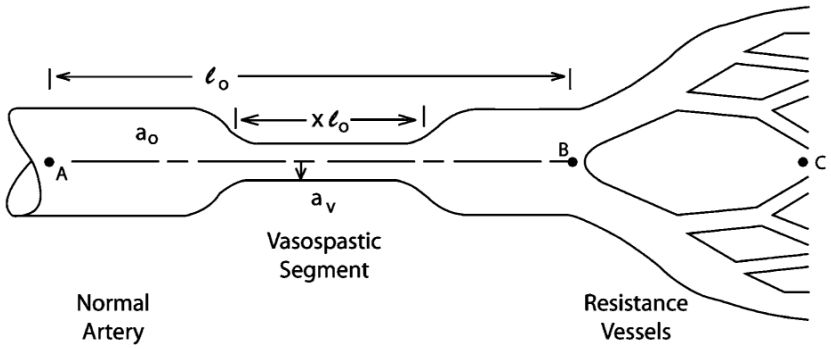

FIGURE 3.

Schema of a segment of a large cerebral artery (e.g., middle cerebral) undergoing vasospasm, with an emphasis on the existence of distal resistance vessels. Noted, too, are dimensions and points along the vessel that are relevant to a 1-D control volume analysis of the altered hemodynamics (luminal pressure and flow). Flow in the large artery can thus be modeled via the pipe flow equation whereas that in the resistance vessels can be modeled via a lumped parameter resistance. Finally, note that the vessel is typically surrounded by cerebrospinal fluid (CSF), which can change over time and exert a pressure on the outer surface of the vessel. Effects of intracranial pressure are probably more marked on the net resistance, however, by collapsing distal venules[36].

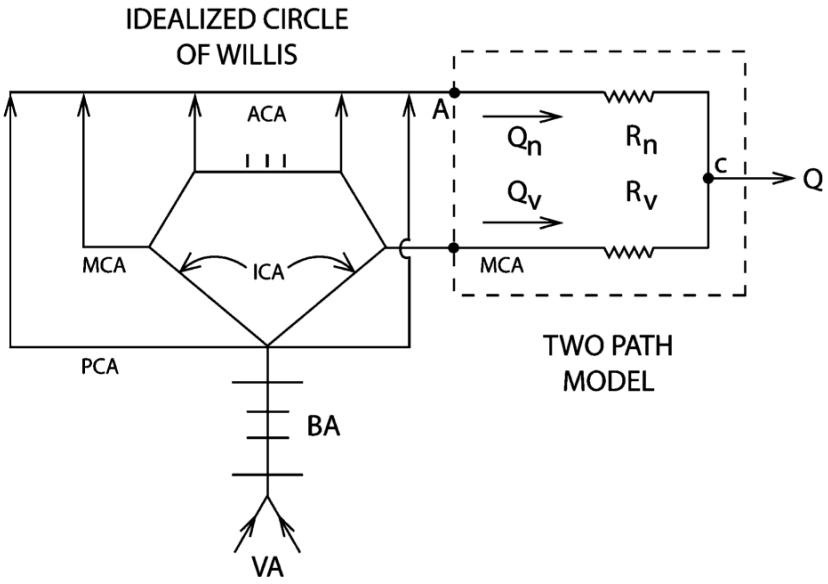

FIGURE 4.

Idealized representation of the cerebral circulation as a "two-path" network.[36] The vasospasm path models a single constricted middle cerebral artery (MCA) and its distal resistance vessels whereas the normal path models all remaining large vessels (e.g., both anterior cerebral arteries ACA, the contralateral middle cerebral artery, and both posterior cerebral arteries PCA) and their associated distal resistance vessels.